

Methoden moderner Röntgenphysik II: Streuung und Abbildung

Lecture 13	Vorlesung zum Haupt- oder Masterstudiengang Physik, SoSe 2017 G. Grübel, <u>A. Philippi-Kobs</u> , O. Seeck, T. Schneider, L. Frenzel, M. Martins, W. Wurth
Location	Lecture hall AP, Physics, Jungiusstraße
Date	Tuesday 12:30 - 14:00 (starting 4.4.) Thursday 8:30 - 10:00 (until 13.7.)

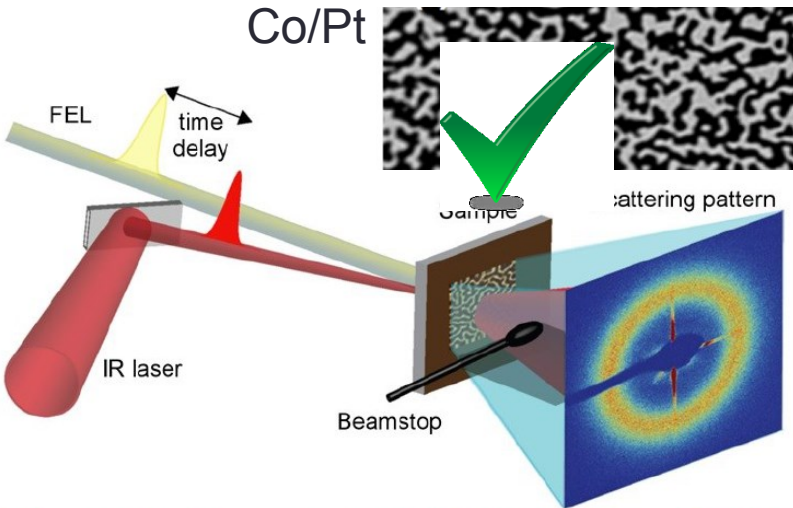
Part II

Magnetism – Magnetic Thin Films

by André Philippi-Kobs (AP)

[23.5.] Magnetic small angle scattering of magnetic domain pat

- Introduction of magnetism in thin films
- Resonant scattering & X-ray magnetic circular dichroism



B. Pfau et al., *Nature Communications*, Vol. 3, 11; DOI:doi:10.1038/ncomms2108 (2012)
 L. Müller et al., *Rev. Sci. Instrum.* 84, 013906 (2013)

[30.5.] Imaging of magnetic domains

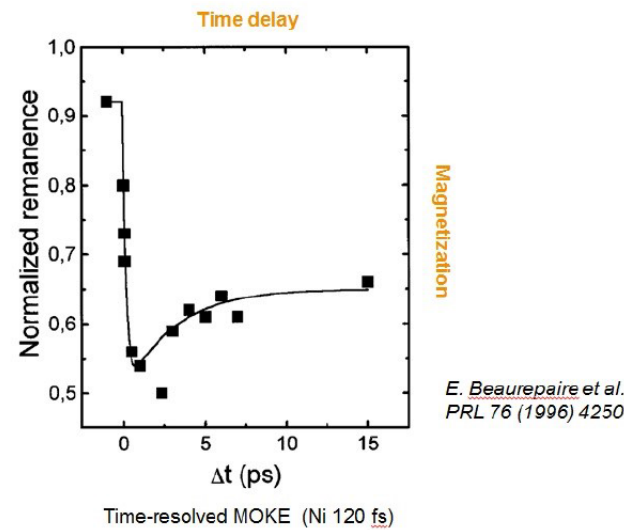
- Fourier transform holography (FTH)
- Scanning transmission X-ray microscopy (STXM)
- Coherent diffraction imaging (CDI), Ptychography

[1.6.] Femtomagnetism

- Introduction of ultrafast magnetization dynamics
- Pump-probe experiments of nano-scale magnetic domain patterns

[13.6.] Related aspects

- Determination of coherence via magnetic domain patterns
- Magnetic XRD of antiferromagnets and chiral systems
- Further electronic inhomogeneities probed by X-rays (charge density wave; Abrikosov vortices in superconductors)



Resonant magnetic small angle X-ray scattering (mSAXS) of magnetic domain patterns

1.) Ferromagnetism in a nutshell

- forms of magnetic phenomena
- contributions to free energy
- focus on systems with perpendicular magnetic anisotropy (Co/Pt multilayers)
- magnetic domains and domain walls

2.) Interaction of **polarized** photons with matter

- Recap: Charge and **Spin** X-ray Scattering by a single electron
- Recap classical concept of Absorption & Resonant Scattering (forced oscillator)
- Absorption and Resonant Scattering (**QM concept**, Fermi's Golden rule)
- Interactions of photons with ferromagnetic materials → XMCD effect
(- XMLinearD and X-ray Natural Dichroism)

3.) Resonant magnetic SAXS of magnetic domain patterns

Interaction of polarized photons with matter

➤ From Absorption to Resonant Scattering (exp. approach):

$$f'' = -(k/4\pi) \sigma_a(E)$$

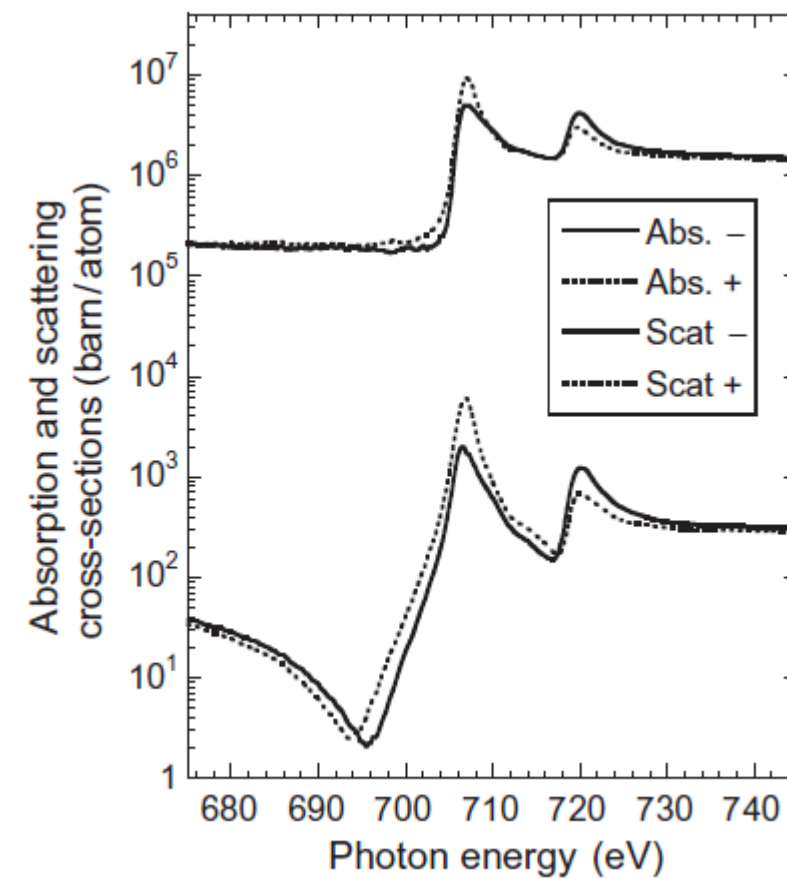
Measure absorption cross-section for both helicities

Kramers-Kronig relation

$$\downarrow f$$

$$\sigma_{\text{scattering}} = f^2$$

$$= [Z + f'(\omega, \epsilon)]^2 + [f''(\omega, \epsilon)]^2$$



Interaction of polarized photons with matter

> Resonant scattering (qm concept): 2. Term of Fermi's Golden rule in dipole approx.

$$T_{if} = \frac{2\pi}{\hbar} \left| \langle f | \mathcal{H}_{\text{int}} | i \rangle + \sum_n \frac{\langle f | \mathcal{H}_{\text{int}} | n \rangle \langle n | \mathcal{H}_{\text{int}} | i \rangle}{\varepsilon_i - \varepsilon_n} \right|^2 \delta(\varepsilon_i - \varepsilon_f) \rho(\varepsilon_f) \quad \sigma = \frac{T_{if}}{\Phi_0}$$

↓ Dipol approximation etc. (as done for absorption term)

$$\frac{\hbar^2 \omega^4}{c^2} \alpha_f^2 \left| \sum_n \frac{\langle a | \mathbf{r} \cdot \boldsymbol{\epsilon}_2^* | n \rangle \langle n | \mathbf{r} \cdot \boldsymbol{\epsilon}_1 | a \rangle}{(\hbar\omega - E_R^n) + i(\Delta_n/2)} \right|^2 \quad \Delta_n: \text{line width}$$

↓ J. P. Hannon et al., Phys. Rev. Lett **61**, 1245 (1988)

$$\begin{aligned} \langle a | \mathbf{r} \cdot \boldsymbol{\epsilon}_2^* | n \rangle \langle n | \mathbf{r} \cdot \boldsymbol{\epsilon}_1 | a \rangle &= \frac{\mathcal{R}^2}{2} [(\boldsymbol{\epsilon}_2^* \cdot \boldsymbol{\epsilon}_1) \{ |C_{+1}|^2 + |C_{-1}|^2 \} \\ &\quad + i(\boldsymbol{\epsilon}_2^* \times \boldsymbol{\epsilon}_1) \cdot \hat{\mathbf{m}} \{ |C_{-1}|^2 - |C_{+1}|^2 \} \\ &\quad + (\boldsymbol{\epsilon}_2^* \cdot \hat{\mathbf{m}})(\boldsymbol{\epsilon}_1 \cdot \hat{\mathbf{m}}) \{ 2|C_0|^2 - |C_{-1}|^2 - |C_{+1}|^2 \}] \end{aligned}$$

Interaction of polarized photons with matter

- Resonant scattering: 2. Term of Fermi's Golden rule in dipole approximation

$$T_{if} = \frac{2\pi}{\hbar} \left| \langle f | \mathcal{H}_{\text{int}} | i \rangle + \sum_n \frac{\langle f | \mathcal{H}_{\text{int}} | n \rangle \langle n | \mathcal{H}_{\text{int}} | i \rangle}{\varepsilon_i - \varepsilon_n} \right|^2 \delta(\varepsilon_i - \varepsilon_f) \rho(\varepsilon_f)$$

with $\sigma = \frac{T_{if}}{\Phi_0}$ and $\sigma_{\text{scattering}} = f^2$

- The *elastic resonant magnetic scattering factor* in units [number of electrons] is given by

$$f(\omega, \boldsymbol{\varepsilon}_1) = \frac{\hbar\omega^2 \alpha_f \mathcal{R}^2}{2cr_0} \left[\underbrace{(\boldsymbol{\epsilon}_2^* \cdot \boldsymbol{\varepsilon}_1) G_0}_{\text{charge}} + \underbrace{i(\boldsymbol{\epsilon}_2^* \times \boldsymbol{\varepsilon}_1) \cdot \hat{\mathbf{m}} G_1}_{\text{XMCD}} + \underbrace{(\boldsymbol{\epsilon}_2^* \cdot \hat{\mathbf{m}})(\boldsymbol{\varepsilon}_1 \cdot \hat{\mathbf{m}}) G_2}_{\text{XMLD}} \right]$$

$$G_1 = \sum_n \frac{|\langle a | C_{-1}^{(1)} | n \rangle|^2 - |\langle a | C_{+1}^{(1)} | n \rangle|^2}{(\hbar\omega - E_R^n) + i(\Delta_n/2)}$$

For circularly polarized light

$$i [(\boldsymbol{\epsilon}^\pm)^* \times \boldsymbol{\epsilon}^\pm] = \mp \mathbf{e}_z$$

Charge: Natural linear dichroism

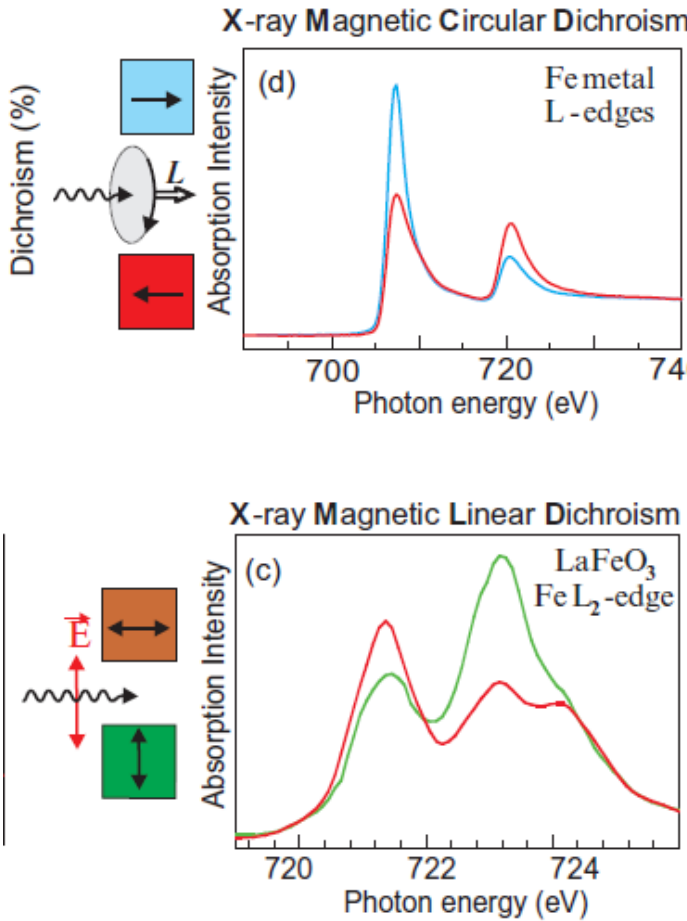
XMLD: X-ray magnetic linear dichroism

$$G_0 = \sum_n \frac{|\langle a | C_{+1}^{(1)} | n \rangle|^2 + |\langle a | C_{-1}^{(1)} | n \rangle|^2}{(\hbar\omega - E_R^n) + i(\Delta_n/2)}$$

$$G_2 = \sum_n \frac{2|\langle a | C_0^{(1)} | n \rangle|^2 - |\langle a | C_{-1}^{(1)} | n \rangle|^2 - |\langle a | C_{+1}^{(1)} | n \rangle|^2}{(\hbar\omega - E_R^n) + i(\Delta_n/2)}$$

Interaction of polarized photons with matter

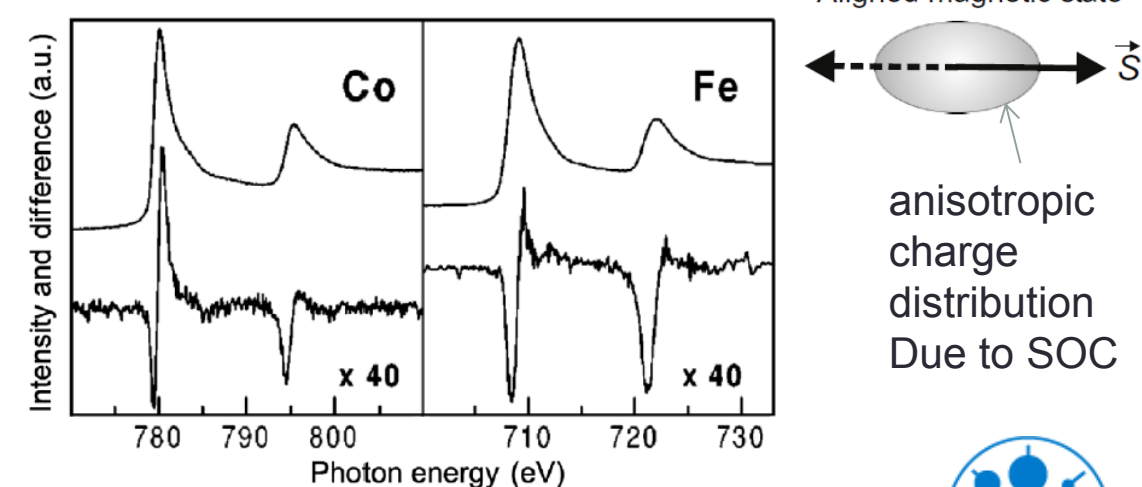
> XMCD and XMLD effect



X-ray “magnetic” dichroism is due to spin alignment and the spin–orbit coupling.

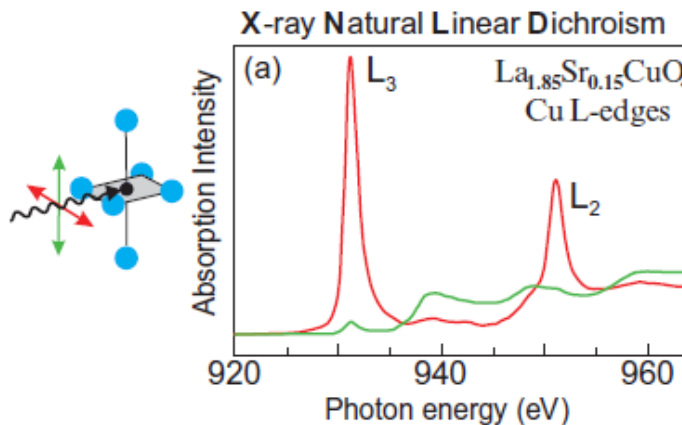
- X-ray magnetic circular dichroism – XMCD – arises from *directional* spin alignment. The effect is parity even and time odd.

- X-ray magnetic linear dichroism – XMLD – arises from a charge anisotropy induced by *axial* spin alignment. The effect is parity even and time even.



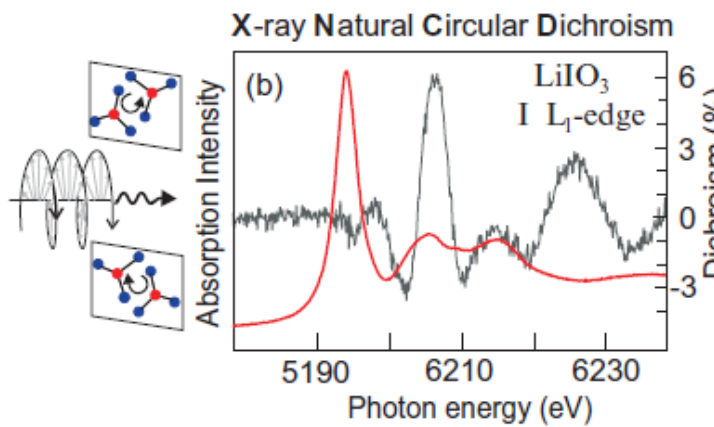
Interaction of polarized photons with matter

> XNLD and XNCD effect

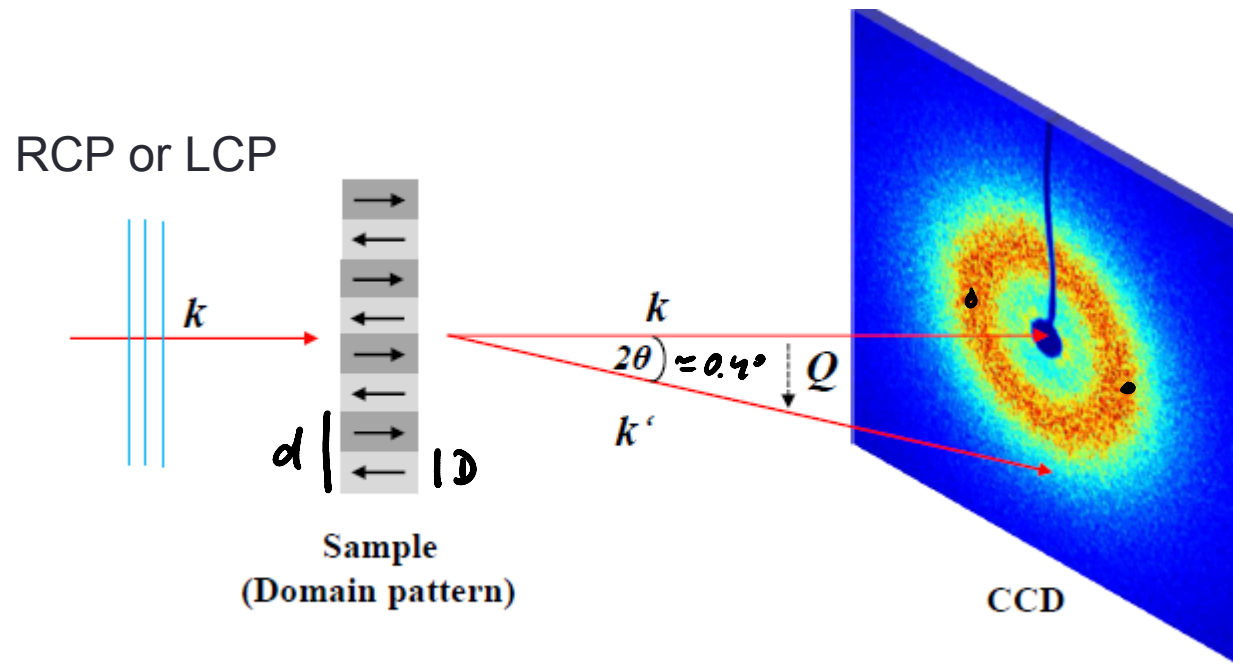


X-ray “natural” dichroism refers to the absence of spin alignment.

- X-ray natural linear dichroism – XNLD – is due to an anisotropic charge distribution. The effect is parity even and time even.
- X-ray natural circular dichroism – XNCD – may be present for anisotropic charge distributions that lack a center of inversion. The effect is parity odd and time even.



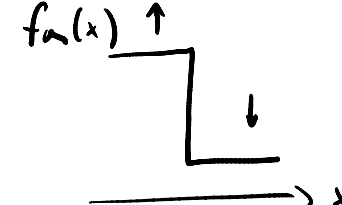
mSAXS of magnetic domain patterns



„magnetic grating/lattice“ = stripe domain pattern with equal domain size D
 (periodicity of $d = 2D$)

→ Scattering factor $f_m = M_z F^m$ varies in x-direction due to XMCD effect & alternating M_z

$$f_m(x) = \underbrace{f_n^*(x)}_{\text{unit cell}} \otimes \underbrace{\sum_{n=-\infty}^{\infty} \delta(x - n d)}_{\text{lattice}}$$



mSAXS of magnetic domain patterns

Scattering amplitude (Fourier transform of scattering factor):

$$A(Q) = \mathcal{F}T(f(n)) = \underbrace{\tilde{f}_n^0(Q)}_{\text{unit cell}} \sum_{n=-\infty}^{\infty} e^{-iQ_n d}$$

with scattering vector (momentum transfer) : $Q = k - k' = \frac{4\pi}{\lambda} \sin \theta$

Scattering intensity:

$$I(Q) = |A(Q)|^2 = \begin{cases} |\tilde{f}_n^0(Q)|^2 \cdot N_d^2 & \text{for } e^{iQ_n d} = 1 \\ \sim 0 & \text{else} \end{cases}$$

1/2 number of domains

① for $Q \cdot d = 2\pi \Rightarrow Q = \frac{2\pi}{d}$

$$d = 200 \text{ nm}$$

$$\Theta = \arcsin\left(\frac{\lambda}{2d}\right) = 0.2^\circ$$

$$\lambda_{\text{c-edges}} \approx 1.5 \text{ nm}$$

Part II

Magnetism – Magnetic Thin Films

by André Philippi-Kobs (AP)

 Magnetic small angle scattering of magnetic domain patterns

Introduction of magnetism in thin films
Resonant scattering & X-ray magnetic circular dichroism (XMCD),

[30.5.] Imaging of magnetic domains

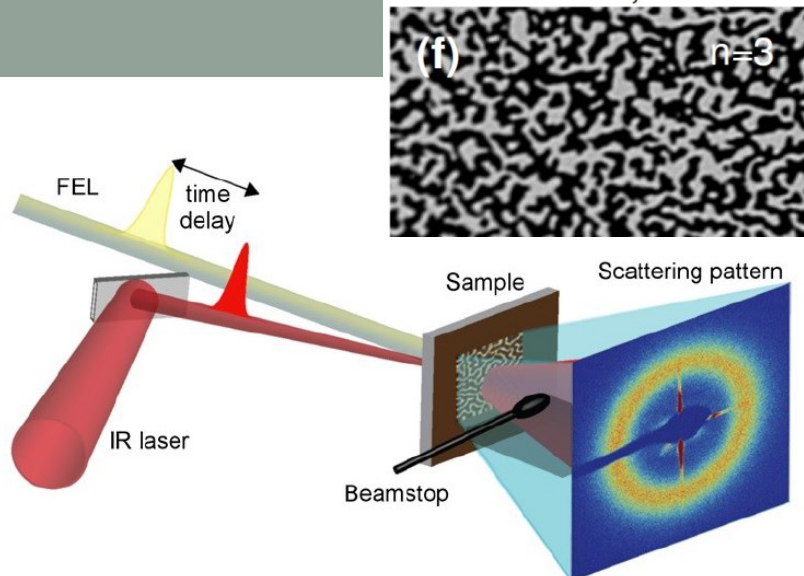
- Fourier transform holography (FTH)
- Scanning transmission X-ray microscopy (STXM)
- Coherent diffraction imaging (CDI), Ptychography

[1.6.] Femtomagnetism

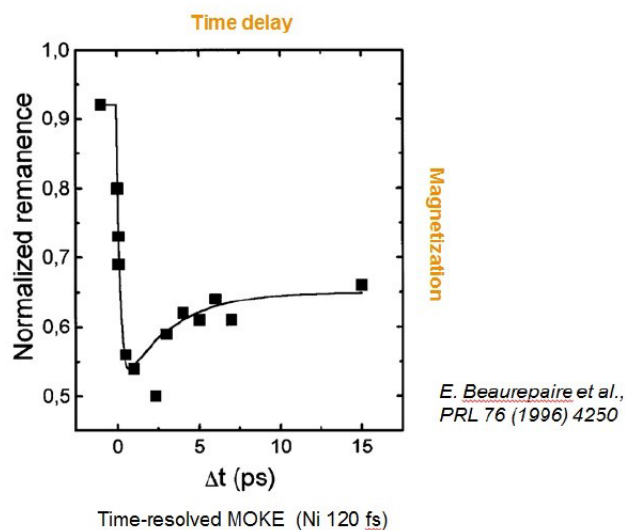
- Introduction of ultrafast magnetization dynamics
- Pump-probe experiments of nano-scale magnetic domain patterns

[13.6.] Related aspects

- Determination of coherence via magnetic domain patterns
- Magnetic XRD of antiferromagnets and chiral systems 
- Further electronic inhomogeneities probed by X-rays (charge density wave; Abrikosov vortices in superconductors)



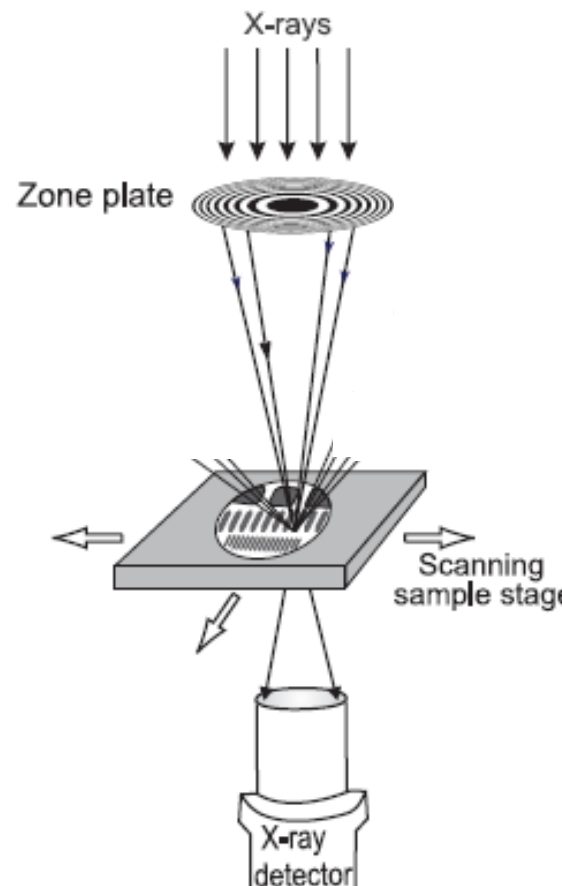
B. Pfau et al., *Nature Communications*, Vol. 3, 11; DOI:doi:10.1038/ncomms2108 (2012)
L. Müller et al., *Rev. Sci. Instrum.* 84, 013906 (2013)



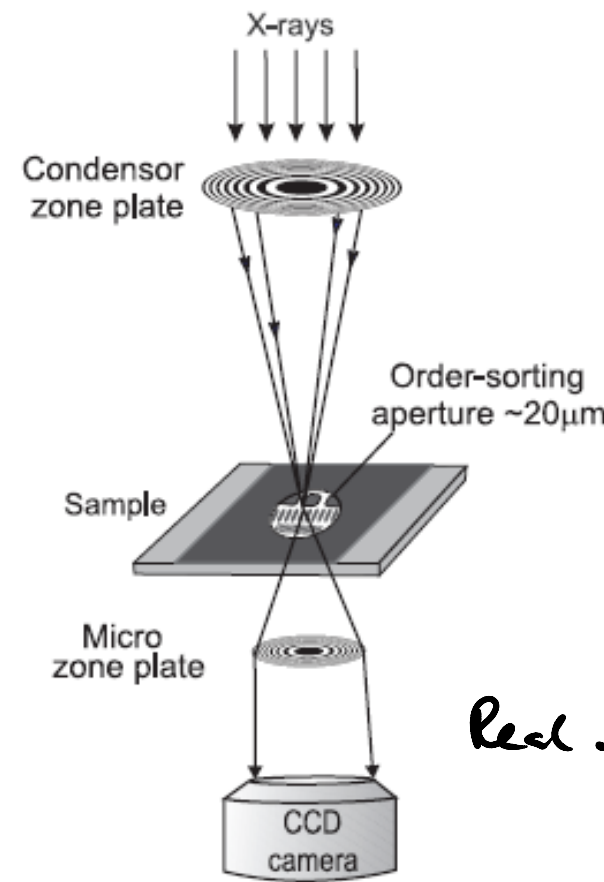
Imaging of magnetic domain patterns with X-rays

> X-ray lenses based methods

Scanning Transmission X-ray Microscopy
STXM



Transmission Imaging X-ray Microscopy
TIXM



Imaging of magnetic domain patterns with X-rays

> X-ray lenses based method

Fresnel Zone plates:

Condition for constructive interference at focus f:

$$r_m = \sqrt{m\lambda f + \frac{m^2\lambda^2}{4}}$$

$$\approx \sqrt{m\lambda f}$$

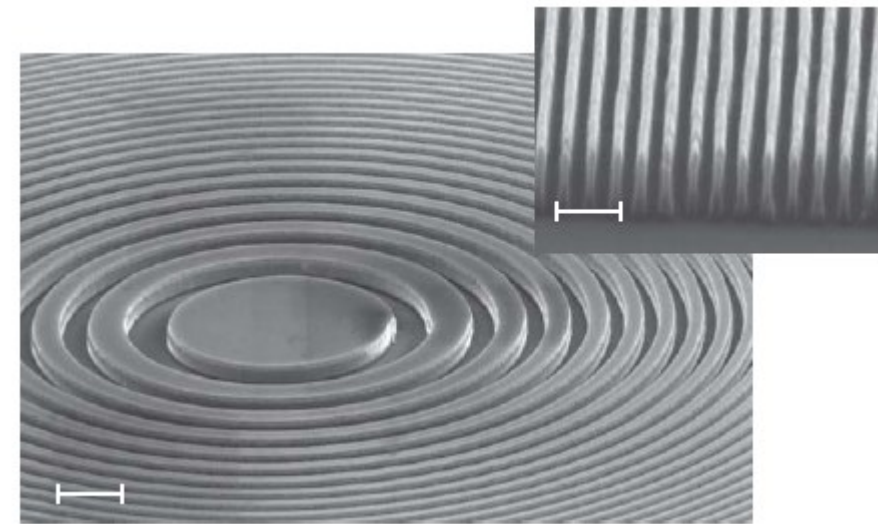
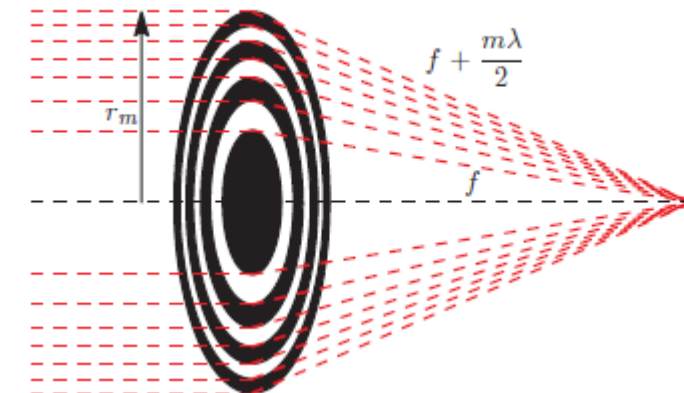
Resolution determined by width of outermost zone Δr_m :

$$\Delta x = 1.22 \Delta r_m$$

$\Delta r_m \gtrsim 10 \text{ nm}$ nowadays

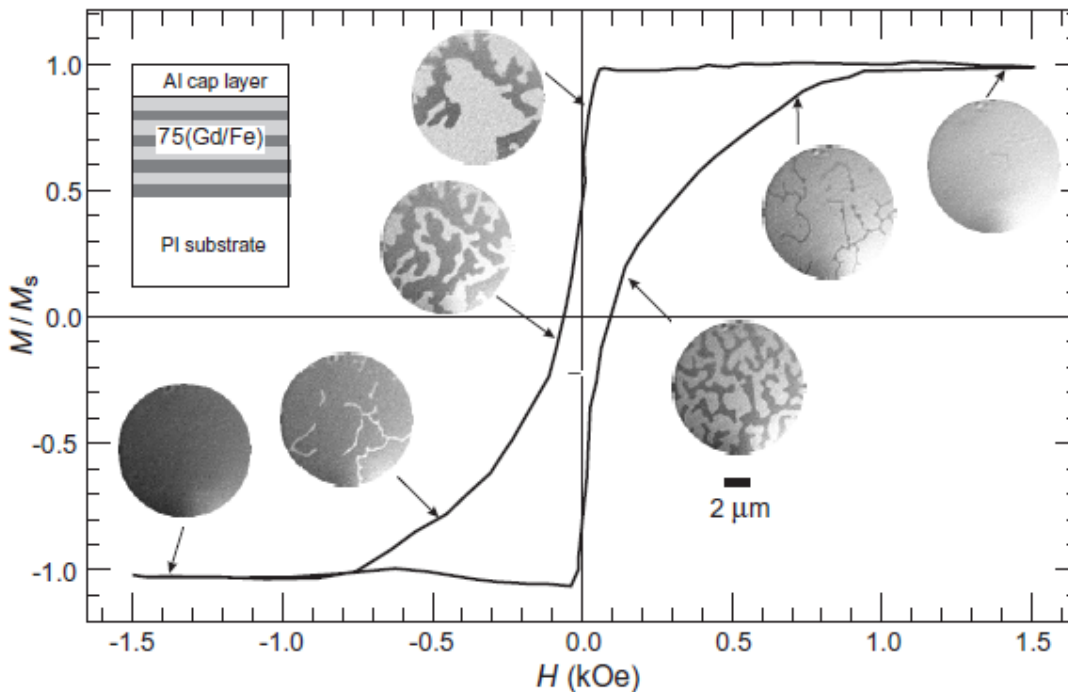
disadvantages:

- High absorption
- Hard to fabricate



Imaging of magnetic domain patterns with X-rays

➤ X-ray lenses based method



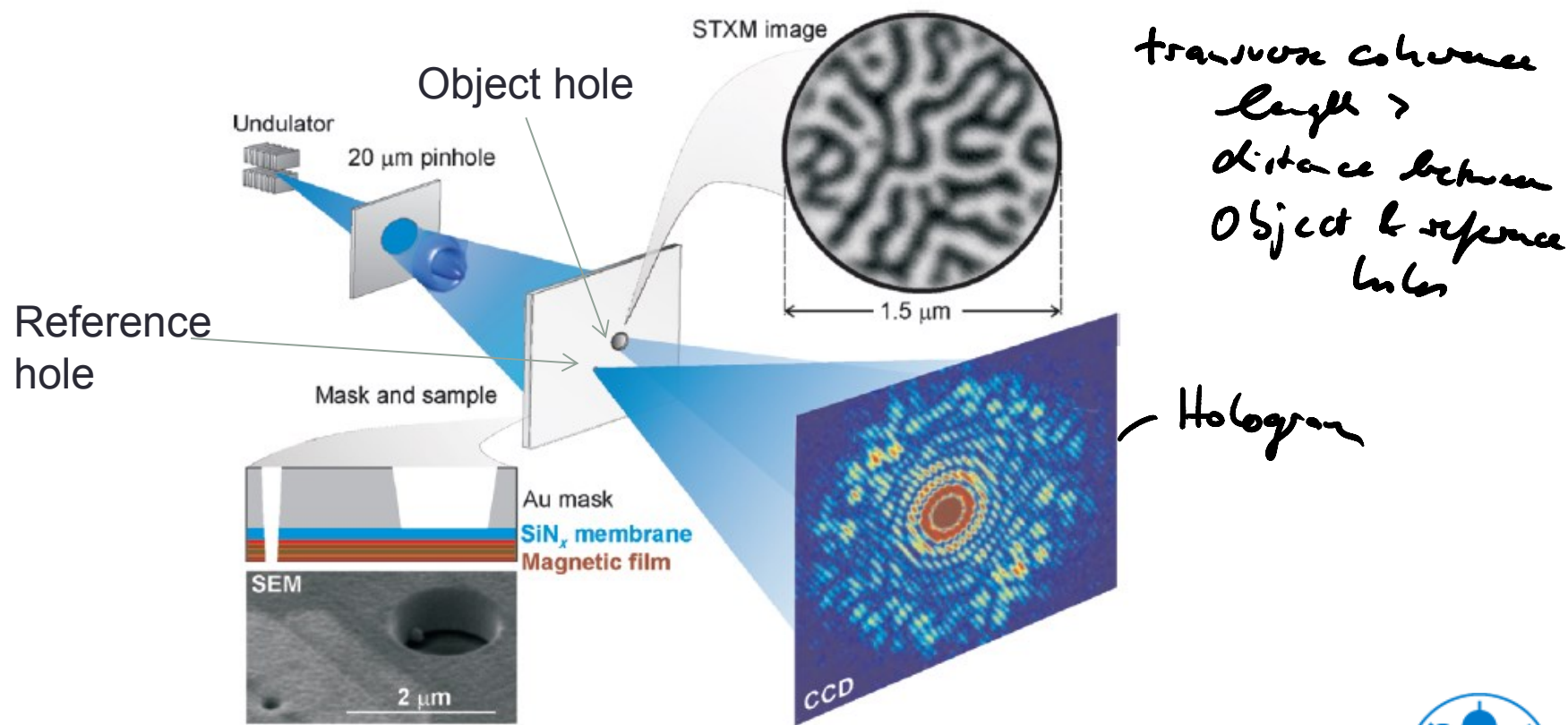
- Element-sensitivity
- Integration of gray values for each field value
→ hysteresis

Fig. 10.22. TIXM images recorded at the FeL₃-edge as a function of applied field for a $75 \times [\text{Fe}(4.1 \text{ \AA})/\text{Gd}(4.5 \text{ \AA})]$ multilayer deposited on polyimide and capped for protection with an Al layer [463, 482]

Imaging of magnetic domain patterns with X-rays

> Lensless Imaging – Fourier transform Holography

	Schlüssellement-Herstellung		Bild-Rekonstruktion	
TXM	Zonenplatte	XXXXX	-direkt-	X
FTH	Optikmaske	XX	Einfache Fourier-Transformation	XX

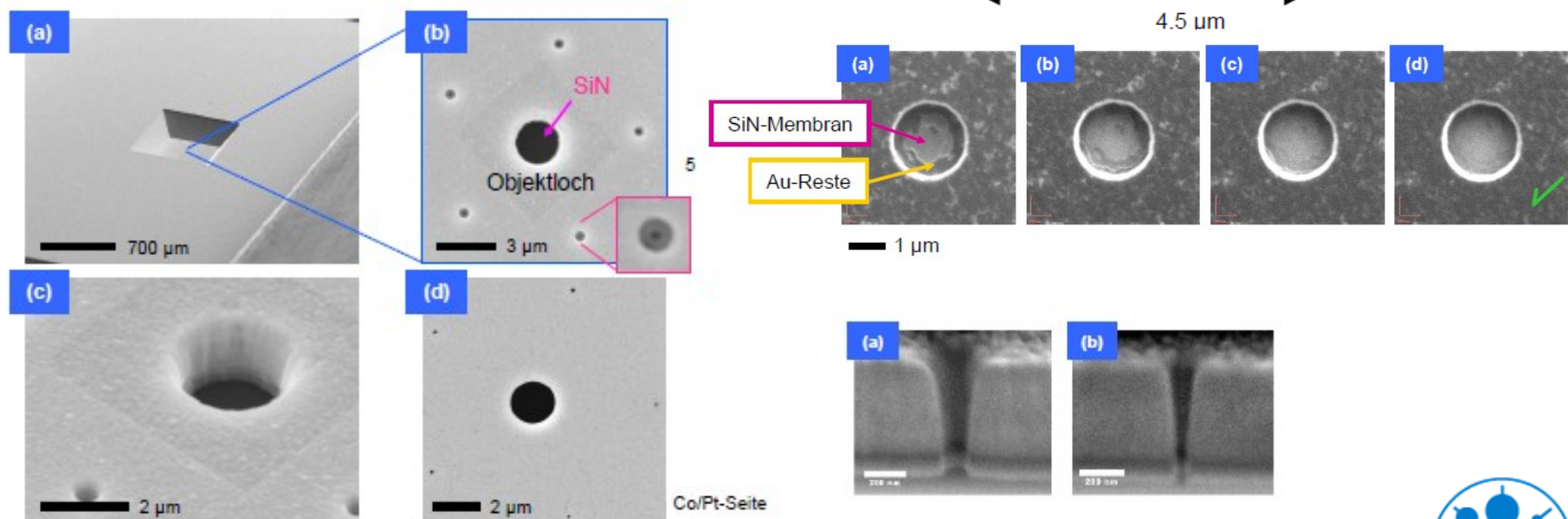
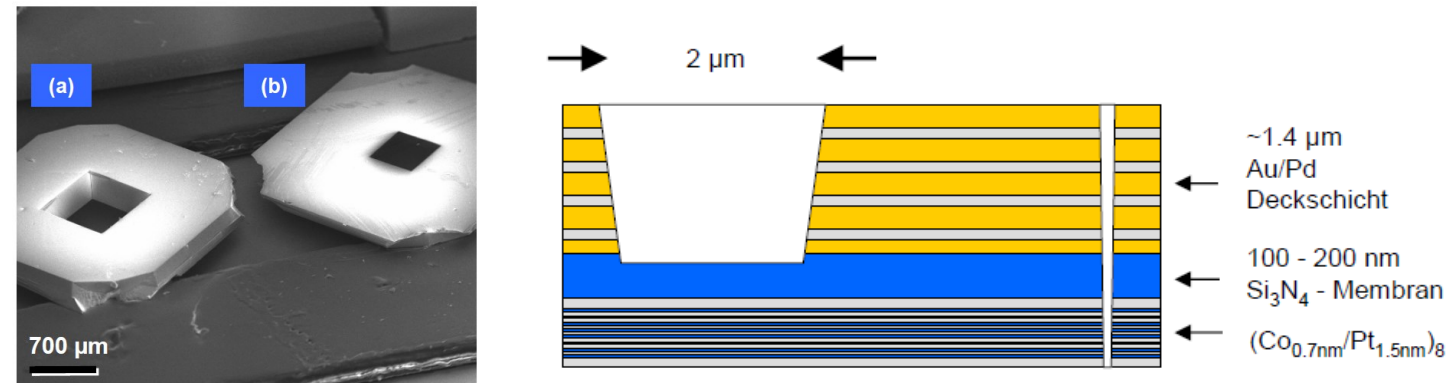


Imaging of magnetic domain patterns with X-rays

> Lensless Imaging – Fourier transform Holography

Mask and sample:

Preparation
by focused ion beam
technique



Imaging of magnetic domain patterns with X-rays

> Lensless Imaging – Fourier transform Holography (FTH)

Principle:

- Intensity on detector: $I(\vec{Q}) = \left| \sum_j f_j(\vec{Q}) e^{i\vec{Q} \cdot \vec{s}_j} \right|^2$

- Scattering factor for circularly polarized light and $\mathbf{M} \parallel \mathbf{L}_{ph}$:

$$f = \vec{\epsilon} \cdot \vec{\epsilon}' F^c - i (\vec{\epsilon} \times \vec{\epsilon}') \cdot \vec{n} F^n$$

$$f = f^c(\vec{Q}) \pm f^n(\vec{Q}) \quad (+RCP, -LCP)$$

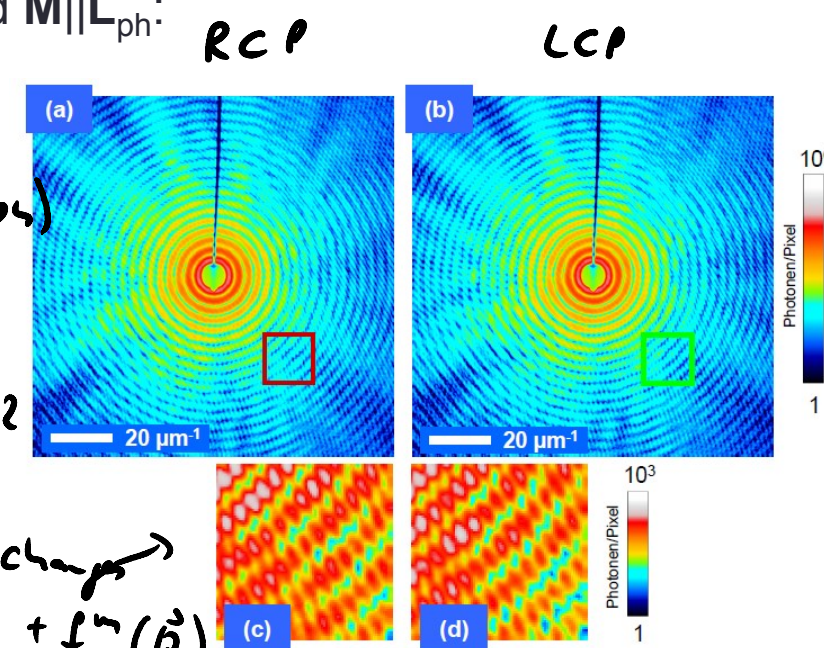
$$f^c(\vec{Q}) = f_0^c(Q) + f_R^c(\vec{Q})$$

- "Hologram" (= $I(\mathbf{Q})$) with RCP and LCP

$$I(\vec{Q}) = |f_0^c(\vec{Q}) + f_R^c(\vec{Q}) \pm f^n(\vec{Q})|^2$$

phase change
due to $\pm f^n(\vec{Q})$

$$\tilde{f}_j(\vec{Q}) = FT(f_j(\vec{r}))$$



Imaging of magnetic domain patterns with X-rays

> Lensless Imaging – Fourier transform Holography (FTH)

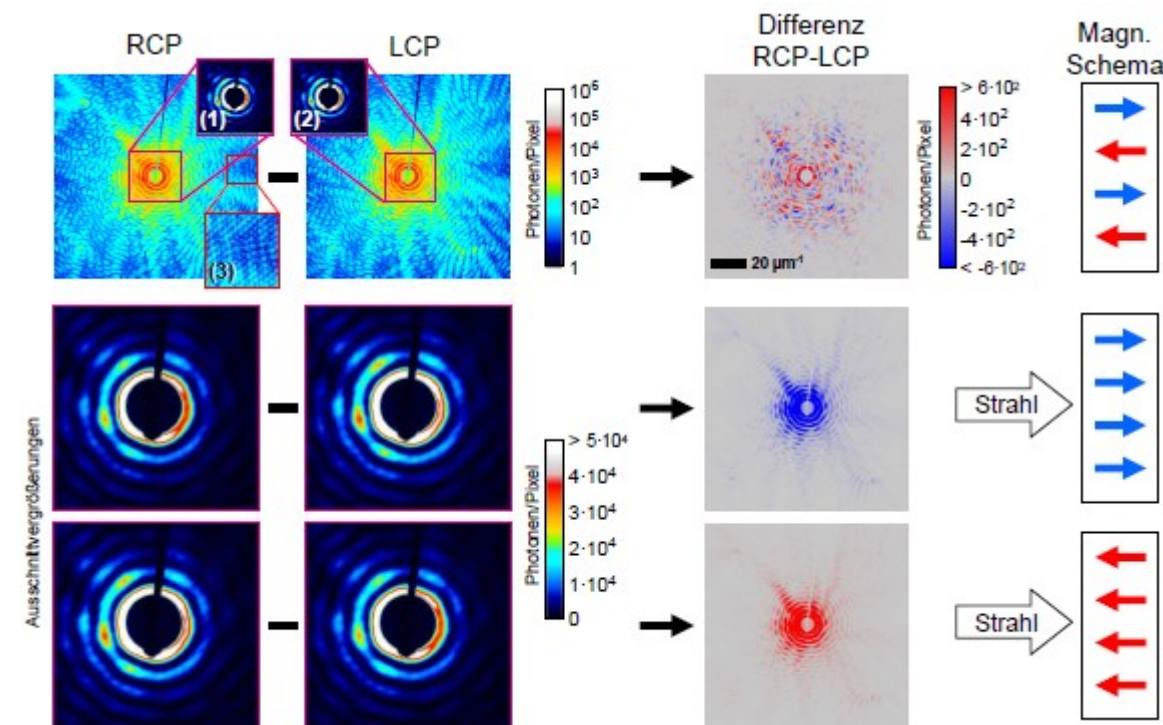
Principle:

- Difference hologram: $\Delta I(\vec{Q})$

$$= I^+(\vec{Q}) - I^-(\vec{Q})$$

$$= \tilde{f}_o^{\perp \times} \cdot \tilde{f}_o^c + \tilde{f}_o^{\perp} \cdot f_o^{\times}$$

$$+ \tilde{f}_o^{\perp \times} \tilde{f}_R^c + \tilde{f}_o^{\perp} \cdot \tilde{f}_R^{\times}$$



Imaging of magnetic domain patterns with X-rays

> Lensless Imaging – Fourier transform Holography (FTH)

Principle: Note: $\widehat{FT}^{-1}(\tilde{f}(\vec{q})) = \widehat{FT}^{-1}\widehat{FT}(f(\vec{r}))$

- Reconstruction = Fourier transformation: $= f(\vec{r})$

$\widehat{FT}^{\gamma}(\Delta I(\vec{q}))$ ^{invers}

$$= \widehat{FT}^{-1}(\tilde{f}_o^{\gamma} \cdot \tilde{f}_o^c) + \widehat{FT}^{-1}(\tilde{f}_o^{\gamma} \cdot \tilde{f}_R^c)$$

Autocorrelation

$$+ \widehat{FT}^{-1}(\tilde{f}_o^{\gamma *} \cdot \tilde{f}_R^c) + \widehat{FT}^{-1}(\tilde{f}_o^{\gamma} \cdot \tilde{f}_R^{c+})$$

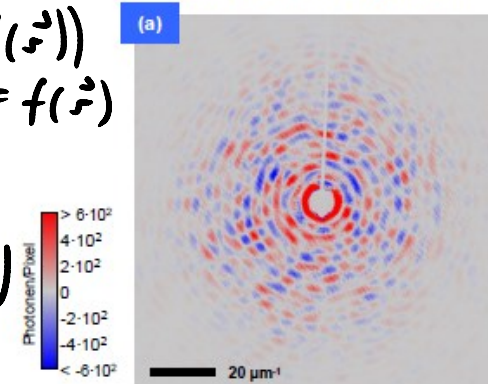
Reconstruction

$$\textcircled{1} = \widehat{FT}^{-1}(\tilde{f}_o^{\gamma}) \otimes \widehat{FT}^{-1}(f_R^{c+})$$

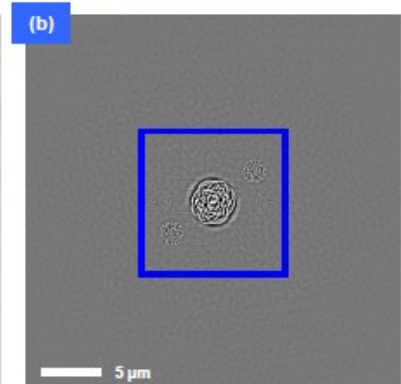
$$= f_o^{\gamma}(\vec{r}) \otimes f_R^{c+}(\vec{r}) \leftarrow \delta - FT\delta$$

$$= \int f_o^{\gamma}(\vec{r}) \delta(\vec{r} - \vec{r}') d\vec{r}' = \underline{\underline{f_o^{\gamma}(\vec{r})}}$$

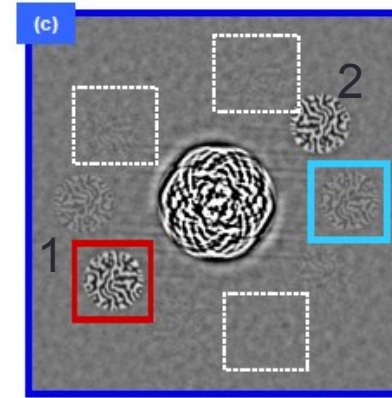
Differenzhologramm



Fourier-Transformation

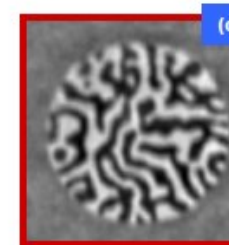


(c)

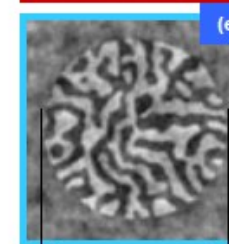


zentraler Ausschnitt

$$R = 57 \text{ nm}$$



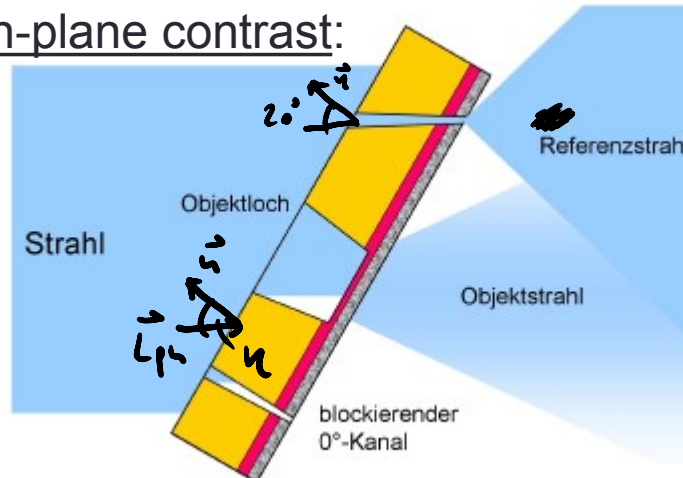
$$R = 30 \text{ nm}$$



Imaging of magnetic domain patterns with X-rays

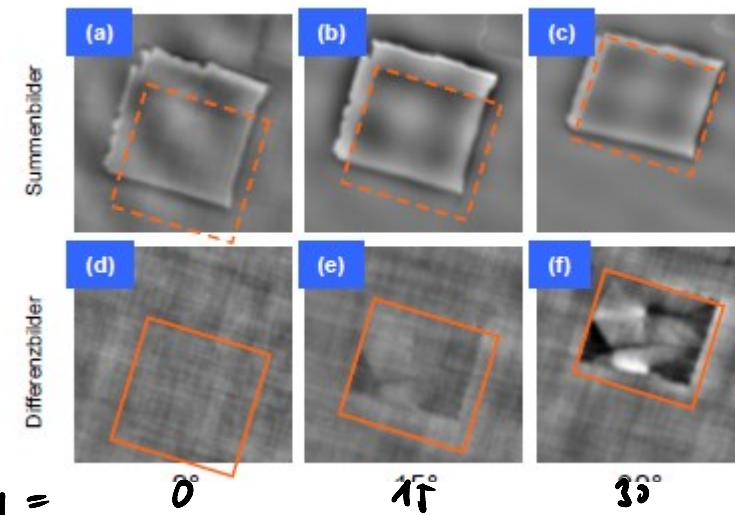
> Lensless Imaging – Fourier transform Holography (FTH)

In-plane contrast:

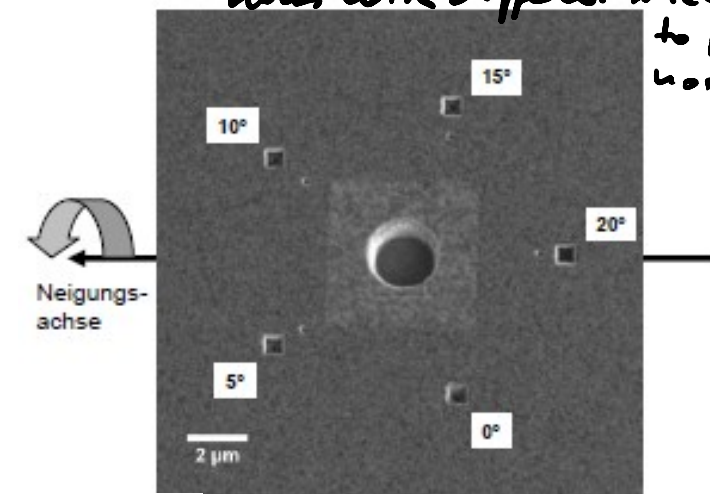


In-plane magnetized
20 nm thick Co film

hole $20^\circ \rightarrow$
inclination



holes with different inclinations
to film normal

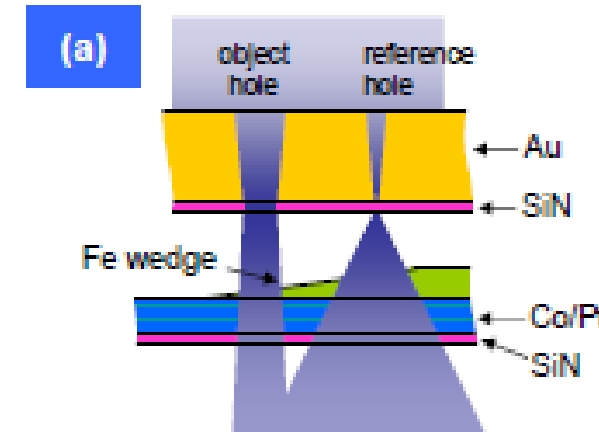
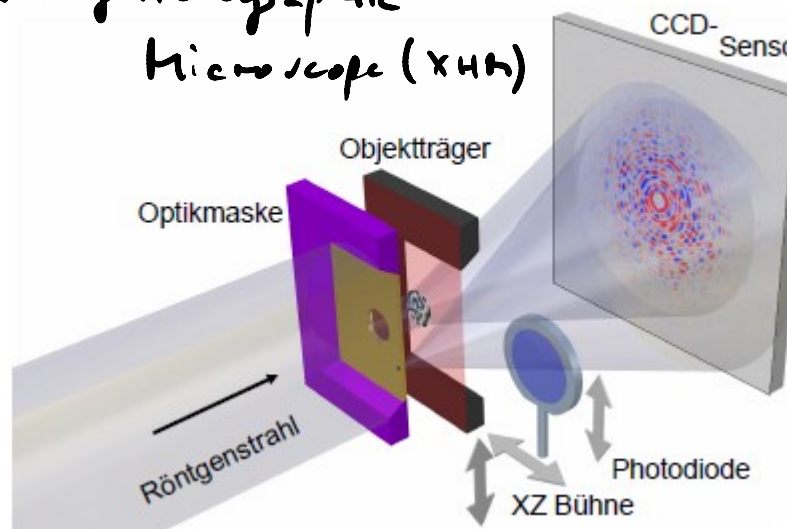


$$\begin{aligned}
 \Delta I_{x\text{ and }y} &\propto \vec{n}_r \cdot \vec{L}_{p\perp} \\
 &= S_h \gamma \cdot \cos \Theta \\
 \gamma &\neq (\vec{L}_{p\perp}, \vec{n}) \\
 \Theta &\neq (\vec{n}_{\parallel p}, \vec{k} \parallel \vec{L}_{p\perp})
 \end{aligned}$$

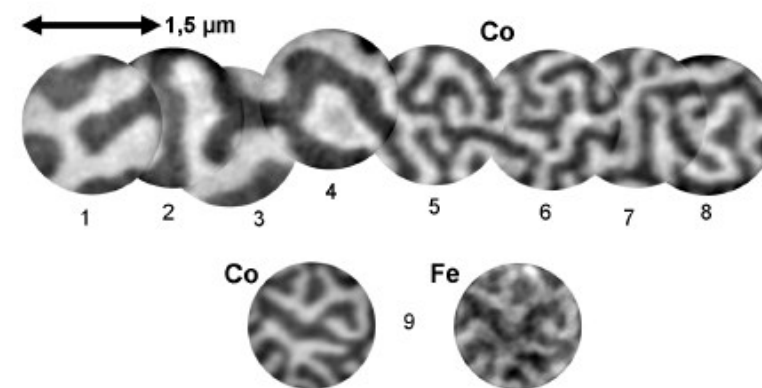
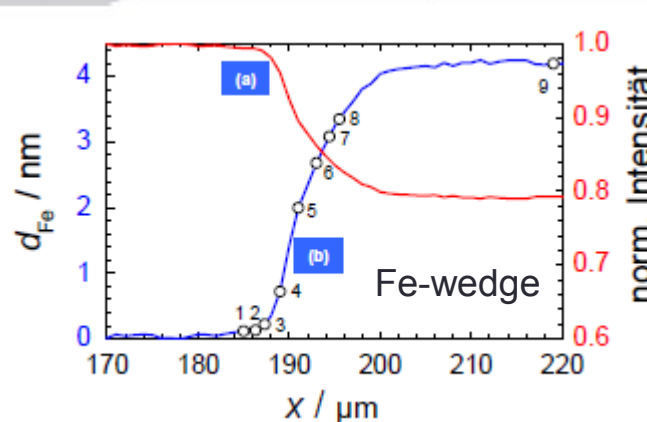
Imaging of magnetic domain patterns with X-rays

> Lensless Imaging – Fourier transform Holography (FTH)

X-ray Holographic Microscope (xHm)



D. Stickler et al., Appl. Phys. Lett. **96**, 042501 (2010)



Element-selectivity

Imaging of magnetic domain patterns with X-rays

> Lensless Imaging – Coherent Diffraction Imaging (CDI)

	Schlüssellement-Herstellung		Bild-Rekonstruktion	
TXM	Zonenplatte	XXXXX	-direkt-	X
FTH	Optikmaske	XX	Einfache Fourier-Transformation	XX
CDI	-direkt-	X	Phasen-Rückgewinnung	XXXXX

